RSC Advances




ROYAL SOCIETY OF CHEMISTRY

www.rsc.org/advances

Cite this: DOI: 10.1039/c0xx00000x

www.rsc.org/xxxxxx

ARTICLE TYPE

# N-substituted defective graphene sheets: Promising electrode materials for Na-ion batteries

**Hao Shen,[a] Dewei Rao,*[a] Xiaoming Xi,[b] Yuzhen Liu,*[c] and Xiangqian Shen[a,b]**

***Received (in XXX, XXX) Xth XXXXXXXXX 20XX, Accepted Xth XXXXXXXXX 20XX***

**DOI: 10.1039/b000000x**

Using density functional theory calculations, we have investigated the adsorption of Na on pristine and N-substituted defective graphene sheets (graphitic, pyridinic, and pyrrolic structures) and explored their application in Na-ion batteries. The adsorption energy and the charge transfer of Na on various types of sheet were calculated. The effects of N-substitution were also studied by electronic structure analysis, including the total electronic density of states, partial electron density of states, and charge density differences. The results show that electron-rich structures have a negative influence on Na binding, while electron-deficient structures are beneficial. The Na storage capacities of different sheets were evaluated by optimizing multiple Na atom adsorbed structures. We found that more Na atoms can be stored on electron-deficient sheets, making them promising for practical application as electrode materials in Na-ion batteries.

## Introduction

The development of novel and efficient energy devices, especially those for energy conversion and storage, becomes more and more important as environmental pollution and the shortage of fossil fuels increase. As an efficient energy carrier system, the Li-ion battery (LIB) has been widely applied as a power source in electric vehicles, cell phone, laptops and so on, owing to its high specific capacity and energy density.[1,2] Nevertheless, the performance of commercial LIBs, by far, cannot satisfy the requirements of large-scale applications. More importantly, global reserves of Li may not be able to meet the enormous expected demands for long-term automotive or large-scale energy storage in the future. Therefore, alternative high performance batteries for powering long-range equipment must be developed. Besides Li, some other metals have been tested in electrode materials for rechargeable batteries, such as Na, K, Ca and Mg.[3-7] Na-ion rechargeable electrochemical cells have been regarded as one of the most promising energy carriers[8] because Na is abundant, low cost, and nontoxic. It also has a suitable redox potential, 2.7 eV versus the standard hydrogen electrode, 0.3 eV higher than that of Li.[9] Therefore, there have been many attempts in recent years to apply Na-containing materials in Na-ion batteries (NIBs), including carbon-based materials,[10-15] metal oxides,[16-18] alloys,[19,20] non-metallic elements,[21,22] and organic compounds.[23,24]

Carbon-based materials are the most common anode candidates for LIBs,[25-27] and are also used in NIBs.[28-32] In recent years, the fantastic properties of two-dimensional (2D) carbon materials have been focused towards many issues. Among these materials, graphene[33] has excellent electrical properties and large specific surface area, which is beneficial for small molecule or atom adsorption,[34] transport,[35] and electrical conductivity.[36] For energy storage, Yoo et al.[37] found that an LIB based on pure graphene exhibited a capacity of 540 mAh/g, and this increased to 730 and 784 mAh/g for samples incorporating carbon nanotubes and fullerenes, respectively. Many works have demonstrated that graphene and its derivatives can be used as electrodes in LIBs.[38-40] Stevens and Dahn[41] studied the insertion mechanisms of Na and Li, and found Li and Na are incorporated into carbon materials in the same way, which means that graphene, as well as its modified structures, should be a promising electrode candidate for NIBs. Experimentally, Wang et al.[42] found that reduced graphene oxide had a reversible capacity as high as 174.3 mAh/g in NIBs. Using first-principles calculations, Datta et al.[43] explored the adsorption of Na atoms on defective graphene, and drew the conclusion that the adsorptive capacity of Na was enhanced by the defective structure. Recently, Yan and coworkers[44] synthesized a sandwich-like porous carbon/graphene composite having a specific capacity of up to 400 mAh/g in NIB, higher than that of Li in graphite, theoretically 372 mAh/g. Importantly, an electrode based on this material had remarkable cycling stability (more than 1000 cycles at 1A/g). More and more works[45-47] have demonstrated that 2D carbon composite materials can be applied as NIB electrodes. However, Na has a larger atomic radius than Li, leading to a lower binding energy and thereby depressing the capacity of the NIB. To avoid these drawbacks, an effective method of strengthening the interactions between Na and carbon materials, which can heavily enhance the Na storage properties as well as the performance of NIBs, is needed.

Various modification methods for enhancing the Li and Na storage capabilities of carbon materials have attracted much attention.[48-52] B and N elements are the most common dopants for

modifying carbon materials because their atomic sizes are the closest to that of carbon. Experimental work has resulted in the successful synthesis of B or N atom substituted graphene.[53] Many reports, both theoretical and experimental, have verified that B and N doped carbon materials have high capacities in LIBs.[54-58] Our previous work[59-62] also explored the influence of B- and N-substitution on Li and Na adsorption in carbon materials, and our computational results showed that the adsorption energy ($E_{ad}$) of Li or Na on B-doped species is higher than that on N-doped ones, and much higher than on pure carbon materials.[61] For Na storage on graphene, Ling et al.[63] studied Na on B-doped graphene via density functional theory (DFT) calculations and declared that the maximum capacity is as high as 762 mAh/g. Wang et al.[64] found that N-doped porous carbon nanosheets in NIBs have a high reversible capacity of 349.7 mAh/g after 260 cycles. Yao et al.[65] studied the adsorption of Na on pristine, B-doped, N-doped, and vacancy graphene, and found that the $E_{ad}$ of Na was increased on B-doped and vacancy species, but decreased on N-doped species. In general, the introduction of heteroatoms into graphene can affect the Na storage, but the effects of N are different on various systems. Therefore, more studies are necessary to explore the mechanisms of Na adsorption on N-doped structures, and will provide further guidance for the design of high performance electrode materials for NIBs.

In this work, pristine and three N-doped defective graphene sheets (graphitic, pyridinic, and pyrrolic graphene, abbreviated as GG, PIG, and PRG, respectively) are studied[66,67]. Their structures are displayed in Scheme 1. To explore the adsorption mechanism of Na on the N-doped species, we systematically studied the influence of N on their geometric and electronic structures, as well as on the C atoms. Finally, the storage capacities of Na on these sheets were assessed.

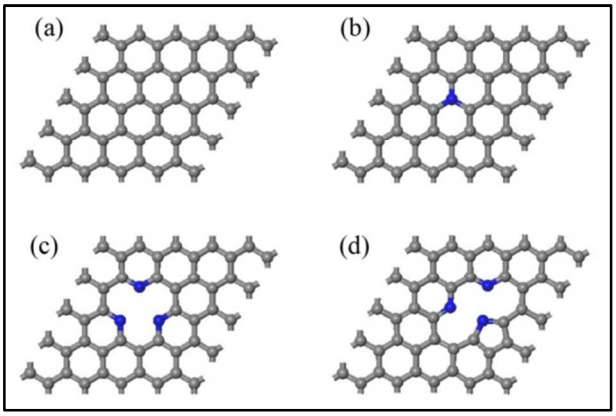


**Scheme 1** Geometric models of (a) pristine graphene, (b)GG, (c)PIG, (d)PRG. Grey balls: C atoms; blue balls: N atoms.

## Computational Methods

All calculations were performed within DFT framework as implemented in DMol$^3$ code[68,69] and the Vienna *ab initio* simulation package (VASP).[70] The generalized gradient approximation with the Perdew-Burke-Ernzerhof functional was employed to describe exchange and correlation effects.[71] For DMol$^3$ calculations, the all electron relativistic core treatment method was implemented for relativistic effects, which explicitly includes all electrons and introduces some relativistic effects into the core. The double numerical atomic orbital augmented by a polarization function was chosen as the basis set,[68] and the spin-unrestricted method was also considered. To ensure high-quality results, the real-space global orbital cutoff radius was set as high as 5.2 Å in the computations. The convergence tolerance of energy was $1.0 \times 10^{-5}$ Ha, the maximum force was $2 \times 10^{-3}$ Ha/Å, and the maximum displacement was $5 \times 10^{-3}$ Å in the geometry optimization. In this work, we chose $5 \times 5 \times 1$ graphene supercells as the computational models, and a vacuum of 18 Å was included in the isolate graphene sheets to reduce the interactions between pairs of sheets.

For VASP, the electron wave functions were expanded in plane waves with an energy cutoff of 500 eV with *k*-mesh grids of $5 \times 5 \times 1$, and the convergence thresholds were set to $10^{-5}$ eV in energy and $10^{-2}$ eV/Å in force. In this work, the density of states (DOS), partial DOS (PDOS) and the charge density differences were calculated by this package.

The $E_{ad}$ of Na on N-doped graphene was calculated by

$$E_{ad}=(E_{nNa+N\text{-}graphene}-nE_{Na}-E_{N\text{-}graphene})/n \quad \text{(EQ.1)}$$

where n is the number of Na atoms, and $E_{nNa+N\text{-}graphene}$, $E_{Na}$ and $E_{N\text{-}graphene}$ are the total energies of the adsorption systems, isolate Na atoms and the N-doped graphene, respectively.

The charge density differences ($D_{cdd}$) for Na adsorption were calculated using the following equation:

$$D_{cdd}=D_{Na+N\text{-}graphene}-D_{Na}-D_{N\text{-}graphene} \quad \text{(EQ.2)}$$

in which $D_{cdd}$ is the charge density difference and $D_{Na+N\text{-}graphene}$, $D_{Na}$ and $D_{N\text{-}graphene}$ are the electron densities of the adsorption systems, isolate Na atoms and the N-doped graphene, respectively.

## Results and Discussion

### Adsorption Mechanism

Experimentally, it has been demonstrated that GG, PIG, and PRG can be synthesized using hydrothermal or chemical vapour deposition methods.[66,67] Based on these works, the geometric structures of each were built (in Scheme 1), and optimized by DFT as shown in Fig. S1 (see the Electronic Supplementary Information, ESI†). As mentioned above, the nature of Na adsorption on N-doped structures is not very clear, including on these N-substituted graphene sheets. To understand the influence of N doping on Na adsorption, we firstly calculated one Na on pristine and N-containing graphene sheets, as displayed in Fig. 1. On pristine graphene, Na prefers to stay at the centre of a carbon hexagon, at a distance of 2.72 Å from each of the nearest six carbons, and 2.32 Å above the plane (details shown in Fig. S2, ESI†), which agrees well with previous reports.[57,65] For GG, single Na is also adsorbed above the hexagonal ring but slightly off centre, 2.97 Å away from the N, an average of 2.59 Å from the nearest carbon atom, and 2.36 Å above the GG surface. In general, the distance between N and a surface can reflect their interaction. The shorter the distance, the stronger the interaction, which means that the binding of Na on graphene should be slightly stronger than that on GG. For defective graphene sheets, Na is likely sited on top of the three-N triangle, 2.28 Å from each N atom and 1.70 Å from the surface of PIG, and an average of

2.37 Å from the three N atoms and 1.83 Å from the surface of PRG. It is clear that the Na atom is closest to the PIG structure, from which we infer that the interaction between Na atoms and PIG is strongest. DFT results show that the $E_{ad}$ of Na is 1.28 eV on GG, lower than on pristine graphene (1.36 eV), 3.33 eV on PRG, and 3.70 eV on PIG. We have previously demonstrated that charge transfer is responsible for the interactions between metal atoms and carbon materials.[72] Next, using Bader population analysis, we collected the charge transfer from Na to host materials (Table 1), and found that GG gains less charge from Na atom than pristine graphene, whereas PIG and PRG sheets can gain much more charge from Na atom than the defect-free graphene sheets, which can heavily affect the interaction energies. These findings indicate that electron-richness (GG) has a negative effect on Na adsorption, resulting in a lower $E_{ad}$ and a possibly lower Na storage capacity, which has been observed in previously published work.[65] In contrast, PIG and PRG are electron-deficient materials, owing to the defects in their structures, and can therefore attract more electrons from Na, leading to higher $E_{ad}$. More details of the charge distributions are displayed in Fig. S3 (ESI†).

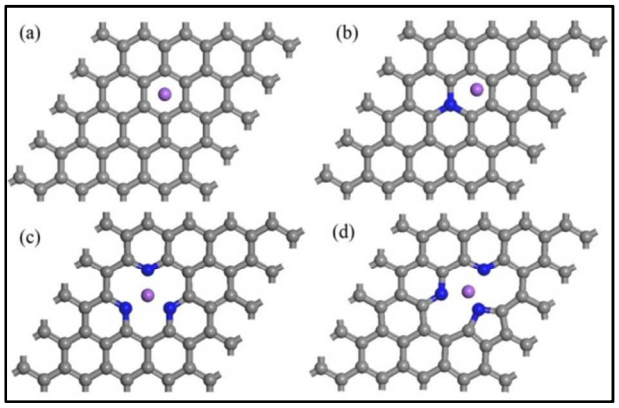


**Fig. 1** Schematic view of the most stable sites of single Na atom adsorbed on (a)pristine graphene and three types of N-doped graphene sheets: (b)GG, (c)PIG, (d)PRG. Grey represent C atoms, blue represent the N atoms and purple represent Na atoms.

**Table 1** The charge (Q) transfer from the adsorbed Na atom to the pristine graphene and GG, PIG, PRG.

| | Most stable site | Q (e) |
|---|---|---|
| pristine | center of hollow site | 0.768 |
| GG | hollow site | 0.765 |
| PIG | center of defect | 0.804 |
| PRG | center of defect | 0.791 |

To further discuss the mechanism of Na adsorption on pristine graphene and N-doped sheets, the total electronic density of states (DOS) of the host materials, and the partial density of states (PDOS) and charge differences of Na adsorbed structures were calculated by VASP. From the DOS of the host materials, as shown in Fig. 2, it is clear that pristine graphene is semi-metallic and has zero gap at the Fermi level (Fig. 2(a)), consistent with previous work.[36] For the N doped GG, the major band features move towards the valance band and the Fermi level is shifted to the conduction band, as shown in Fig. 2(b), which means that GG is an n-type doped material, an electron-rich material, and has little attraction for additional electrons. Fig. 2(c) and (d) show the DOS of PIG and PRG, which are different from that of GG; the major band features of PIG and PRG are moved to the conduction band and the Fermi level is slightly moved towards the valance band, which means that these two materials can attract more electrons on their defective sites. These data agree well with previous work.[73] Additionally, it should be noted that there are three dangling bonds in PIG or PRG at the N atom sites, from which we also can draw the conclusion that both PIG and PRG have electron adsorption ability. Thus, we have demonstrated that the DOS as well as the band profile can be tuned by N doping.

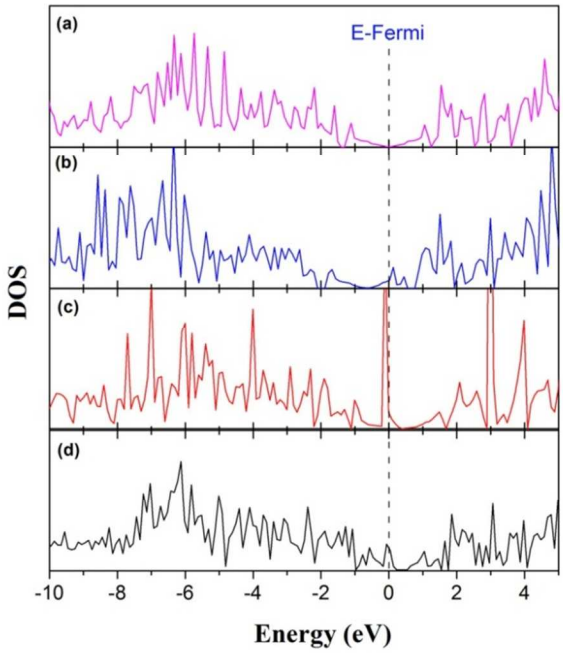


**Fig. 2** Total electronic density of states (DOS) for (a) pristine graphene, (b)GG, (c) PIG and (d) PRG. The dashed line at zero indicates the Fermi level.

Although previous studies have demonstrated that N doped structures have some effect on metal doping, the influence of C and N in N-doped defective graphene sheets used in Na-ion batteries has not been deeply researched. Thus, we calculated the PDOS of the *s* orbital of Na and the *p* orbitals of C and N, as displayed in Fig 3. It is clear that no obvious orbital hybridization between Na and C or N occurs in Na-doped pristine graphene and GG, which means that the interactions between Na and host materials are not very strong. For the PIG and PRG structures, orbital hybridization between the *p* orbital of N and the *s* orbital of Na is observed around −3 eV, implying that the hybridization contributes to the enhanced Na adsorption. Interestingly, the C *2p* and the Na *2s* also exhibit hybridization in PIG and PRG, as shown in Fig. 3, which means that the C also can influence Na adsorption. Therefore, from the PDOS, we found that the N and C atoms at defective sites are responsible for the higher $E_{ad}$ in PIG and PRG.

Cite this: DOI: 10.1039/c0xx00000x

www.rsc.org/xxxxxx

ARTICLE TYPE

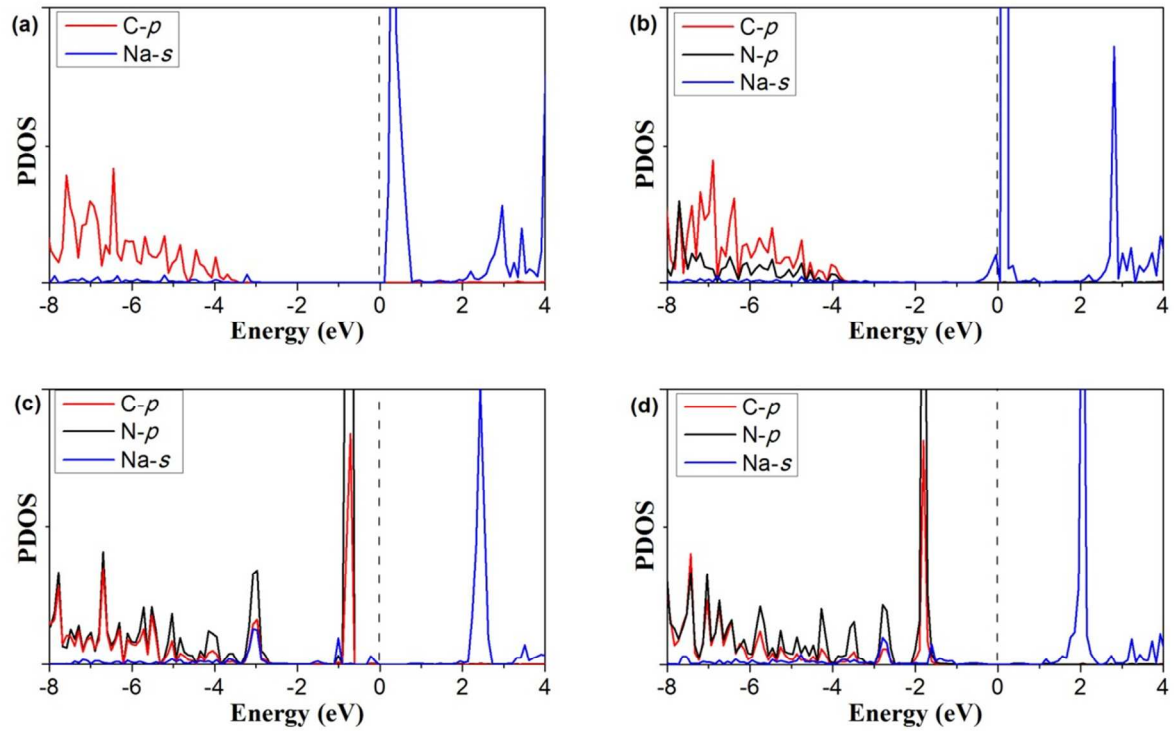


**Fig. 3** The partial density of states (PDOS): (a) Na and C atoms in pristine graphene, (b) Na, N and C atoms in the GG, (c) Na, N and C atoms in the PIG, (d) Na, N and C atoms in the PRG. The dashed line at zero indicates the Fermi level.

To further verify the contribution of C and N, we calculated the charge density differences ($D_{cdd}$), which can provide information on the charge redistribution after Na adsorption and also reflect electrostatic interactions. As displayed in Fig. 4, it is clear that in graphene the electron loss from Na mainly occurs around the six-carbon rings (Fig. 4(a)), which is mainly because the electronegativity of Na is lower than that of the carbon rings. In GG, the accumulation of charge at the six-membered rings is inhomogeneous. Obviously, a greater amount of electron redistribution occurs around N than C, which means that the presence of N in GG can decrease the adsorption of Na. For PIG or PRG, the charge accumulation is mainly centred around N and little dispersed around neighbouring C, which means that in defected graphene the N atoms dominate Coulomb interactions while C also influence the electrostatic interactions. This can be explained as being because the vacancy defects of PIG and PRG break the symmetry of the π-electron system,[33] leading to significant electronic attraction around N in defect holes. We can therefore conclude that charge transfer from Na to N-doped defective graphene sheets influences the binding of Na. Thus, high performance metal storage materials for NIBs, or any other metal-ion batteries, should have an electronic-deficient or highly electronegative structure.

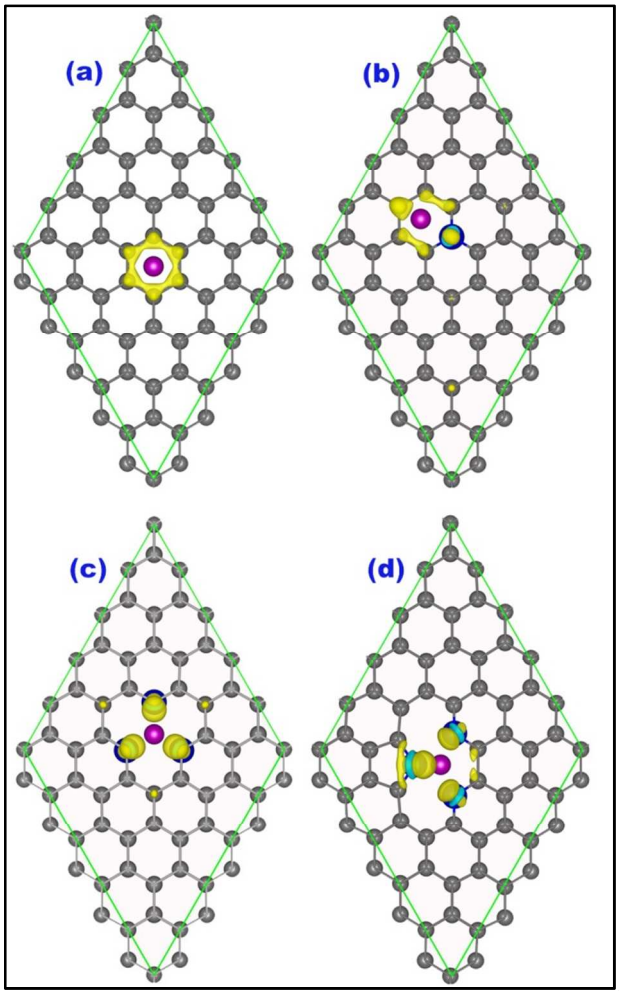


**Fig. 4** The charge density differences for Na adsorption on (a) pristine graphene; (b) GG; (c) PIG and (d) PRG. Purple balls represent Na atoms, blue ones represent N and grey ones are C. yellow: electronic accumulation; cyan: electronic loss.

### Na storage capacity

The key factor of a high performance Na-ion battery material is its Na storage capacity. To evaluate the performance of N-doped graphene nanosheets as electrode materials for NIBs, as well as the influence of N on Na storage, we calculated multiple Na atom adsorption. One to six Na atoms on both sides of N-incorporating structures were studied. The optimized structures are displayed in Fig. 5 and Table S1 (ESI†). In the case of six Na in a supercell structure (Fig. 5), the Na atoms are still adsorbed at hollow sites in pristine graphene but a little off the centre, which could be caused by repulsive interactions between the Na atoms. The distances between the Na and the graphene surface are in the range of 2.78–2.81 Å (Fig. 5(a)). GG is similar to pristine graphene, as shown in Fig. 5(b). In the defective structure of PIG, all Na atoms are adsorbed at defect sites owing to the strong interaction between Na and N atoms, leading to shorter distances between Na and PIG. For PRG, the structure is asymmetric, and the adsorption configuration is changed. As shown in Table S1 (ESI†) and Fig. 5(d), the Na atoms are adsorbed around defect sites when the number of adsorbed Na atoms is greater than three. The Na atoms on PRG are layered, and for six Na, the closest layer is 1.89 Å away from PRG, while the furthest is 3.26 Å away.

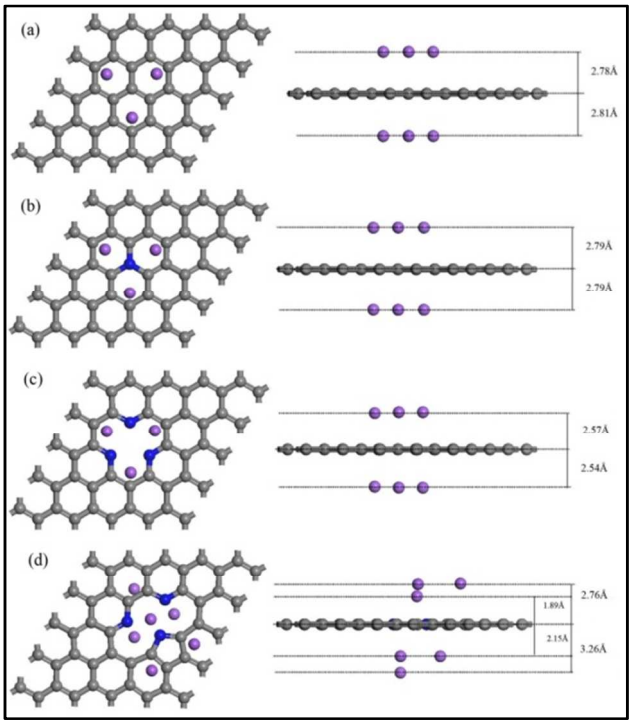


**Fig. 5** The optimization geometries of 6 Na atoms adsorbed on pristine and N-doped graphene. (a) Pristine graphene, (b) GG, (c) PIG, (d) PRG. Left picture show the top view of Na atoms adsorption sites, right picture show the side view and average distance between Na atoms and graphene sheets. Grey represent C atoms, blue represent the N atoms and purple represent Na atoms.

As is well known, the problem of metal clustering in materials is unfavourable for their application in devices like rechargeable cells. We calculated the adsorption energy of Na for multiple Na atoms, and the data are listed in Table 2. Obviously, the $E_{ad}$ decreases with increasing number of Na atoms. Previous works have reported that the cohesive energy of Na is 1.14 eV.[63,65] When the $E_{ad}$ of the host structure is lower than the cohesive energy, the metal atoms tend to aggregate. From Table 2, graphene and GG cannot prevent clustering of Na effectively, and are therefore not suitable for NIBs. Conversely, the average $E_{ad}$ of Na on PIG or PRG is higher than the cohesive energy of Na, even at a high number of adsorbed atoms, up to 6 in the employed supercell, which suggests that PIG and PRG should be excellent electrode materials for NIBs.

**Table 2** The average adsorption energies ($E_{ad}$) of Na atoms on pristine and N-doped graphene sheets.

| Number of Na atom (n) | pristine graphene (eV) | N-doped graphene (eV) | | |
|---|---|---|---|---|
| | | GG | PIG | PRG |
| 1 | - 1.36 | - 1.28 | - 3.70 | - 3.33 |
| 2 | - 1.02 | - 1.00 | - 2.83 | - 2.72 |
| 3 | - 1.07 | - 1.06 | - 2.02 | - 2.01 |
| 4 | - 0.94 | - 0.93 | - 1.65 | - 1.76 |
| 5 | - 0.89 | - 0.89 | - 1.52 | - 1.52 |
| 6 | - 0.93 | - 0.94 | - 1.24 | - 1.41 |

## Conclusions

In summary, we studied the adsorption of Na on pristine and N-substituted structures (GG, PIG, and PRG). DFT calculations were used to obtain the adsorption energy of Na and the charge transfer from Na. The results indicate that the N doped defective structures are beneficial for Na binding and that the charge transfer can significantly influence the adsorption energies. From the DOSs, PDOSs, and $D_{cdd}$, we know that an electron-rich character has a negative effect while electron-deficient structures are beneficial for Na loading, which further verifies that charge transfer is a key factor for Na adsorption. We infer that high performance metal storage materials should have an electronically-deficient or very electronegative structure. Moreover, multiple Na atoms can be efficiently stored on electron-deficient PIG and PRG structures, but not on graphene or GG, which means that defective sheets may be promising electrode materials for application in Na-ion batteries. Theoretical studies have previously demonstrated that the N-doped vacancy graphene sheets could influence the diffusion of Li.[74] But for Na-ion batteries, the influence of defective graphene sheets on Na diffusion is not clear and more work should be devoted to the study of the dynamics of Na during charge/discharge processes.

**Acknowledgements**

This work was financially supported by the National Natural Science Foundation of China (Grant No. 51474113，51474037，51274106, 21403111), the Science and Technology Support Program of Jiangsu Province (Grant No. BE2012143, BE2013071), the Jiangsu Province's Postgraduate Cultivation and Innovation Project (Grant CXZZ13_0662), and Jiangsu Province Science Foundation for Youths (Grant No. BK20140526, BK2012394), China Postdoctoral Science Foundation funded project (Grant No. 2014M561576), and the Research Foundation for Advanced Talents of Jiangsu University (Grant No. 13JDG100).

**Notes and references**

[a] Institute for Advanced Materials, School of Materials Science and Engineering, Jiangsu University, Zhenjiang 212013, P. R. China. E-mail: dewei@ujs.edu.cn.

[b] Changsha Research Institute of Mining and Metallurgy Co., Ltd, No. 966 South Lushan Road, Changsha, 410012, P. R. China.

[c] Department of Applied Physics, Nanjing University of Science and Technology, Nanjing 210094, PR China. E-mail：yzliu@njust.edu.cn.

† Electronic Supplementary Information (ESI) available: details of any supplementary information available should be included here. See DOI: 10.1039/b000000x/

[1] B. Scrosati and J. Garche, *J. Power Sources*, 2010, **195**, 2419.

[2] C. Liu, F. Li, L.P. Ma and H. M. Cheng, *Adv. Mater.*, 2010, **22**, 28.

[3] B. L. Ellis and L. F. Nazar, *Curr. Opin. Solid. St. M.*, 2012, **16**, 168.

[4] M. Hayashi, H. Arai, H. Ohtsuka and Y. Sakurai, *J. Power Sources*, 2003, **119-121**, 617.

[5] D. Aurbach, Z. Lu, A. Schechter, Y. Gofer, H. Gizbar, R. Turgeman, Y. Cohen, M. Moshkovich and E. Levi, *Nature*, 2000, **407**, 12.

[6] A. Eftekhari, *J. Power Sources*, 2004, **126**, 221.

[7] B. Dunn, H. Kamath and J. M. Tarascon, *Science*, 2011, **334**, 928.

[8] S. W. Kim, D. H. Seo, X. H. Ma, G. Ceder and K. Kang, *Adv. Energy Mater.*, 2012, **2**, 710.

[9] S. P. Ong, V. L. Chevrier, G. F. Hautier, A. Jain, C. Moore, S. Kim, X. H. Ma and G. Ceder. *Energy Environ. Sci.*, 2011, **4.9**, 3680.

[10] J. Zhao, L. W. Zhao, K. Chihara, S. Okada, J. Yamaki, S. Matsumoto, S. Kuze and K. Nakane, *J. Power Sources*, 2013, **244**, 752.

[11] C. Luo, Y. Zhu, Y. H. Xu, Y. H. Liu, T. Gao, J. Wang and C. S. Wang, *J. Power Sources*, 2014, **250**, 372.

[12] K. Tang, L. J. Fu, R. J. White, L. H. Yu, M. M. Titirici, M. Antonietti and J. Maier, *Adv. Energy Mater.*, 2012, **2**, 873.

[13] J. Ding, H. L. Wang, Z. Li, A. Kohandehghan, K. Cui, Z. W. Xu, B. Zahiri, X. H. Tan, E. M. Lotfabad, B. C. Olsen and D. Mitlin, *ACS Nano*, 2013, **7**, 11004.

[14] Y. Wen, K. He, Y. J. Zhu, F. D. Han, Y. H. Xu, I. Matsuda, Y. Ishii, J. Cumings and C. S. Wang, *Nat. Commun.*, 2013, **5**, 4033.

[15] Y. Matsuo and K. Ueda, *J. Power Sources*, 2014, **263**, 158.

[16] L.J. Wang, K. Zhang, Z. Hu, W. C. Duan, F. Y. Cheng and J. Chen, *Nano Res.*, 2014, 7, 199.

[17] S. Hariharan, K. Saravanan and P. Balaya, *Electrochem. Commun.*, 2013, **31**, 5.

[18] D.Y. Park and S. T. Myung, *ACS Appl. Mater. Interfaces*, 2014, **6**, 11749.

[19] M. K. Dattaa, R. Epur, P. Saha, K. Kadakia, S. K. Park and P. N. Kumta, *J. Power Sources*, 2013, **225**, 316.

[20] Y. D. Zhang, J. Xie, T. J. Zhu, G. S. Cao, X. B. Zhao and S. C. Zhang, *J. Power Sources*, 2014, **247**, 204.

[21] J. F. Qian, X. Y. Wu, Y. L. Cao, X. P. Ai and H. X. Yang, *Angew Chem. Int. Ed.*, 2013, **52**, 4633.

[22] Y. J. Kim, Y. Park, A. Choi, N. S. Choi, J. Kim, J. Lee, J. H. Ryu, S. M. Oh and K. T. Lee, *Adv. Mater.*, 2013, **25**, 3045.

[23] K. Sakaushi, E. Hosono, G. Nickerl, T. Gemming, H. S. Zhou, S. Kaskel and J. Eckert, *Nat. Commun.*, 2013, **4**, 1485.

[24] Y. Park, D. S. Shin, S. H. Woo, N. S. Choi, K. H. Shin, S. M. Oh, K. T. Lee and S. Y. Hong, *Adv. Mater.*, 2012, **24**, 3562.

[25] M. Winter, J. O. Besenhard, M. E. Spahr and P. Novμk, *Adv. Mater.*, 1998, **10**, 10.

[26] A. Manthiram, *J. Phys. Chem. Lett.*, 2011, **2**, 176.

[27] L. W. Ji, Z. Lin, M. Alcoutlabi and X. W. Zhang, *Energy Environ. Sci.*, 2011, **4**, 2682.

[28] S. Komaba, W. Murata, T. Ishikawa, N. Yabuuchi, T. Ozeki, T. Nakayama, A. Ogata, K. Gotoh and K. Fujiwara, *Adv. Funct. Mater.*, 2011, **21**, 3859.

[29] Y. L. Cao, L. F. Xiao, M. L. Sushko, W. Wang, B. Schwenzer, J. Xiao, Z. Nie, L. V. Saraf, Z. G. Yang and J. Liu, *Nano Lett.*, 2012, **12**, 3783.

[30] V. L. Chevrier and G. Ceder, *J. Electrochem. Soc.*, 2011, **158**, 1011.

[31] V. Palomares, P. Serras, I. Villaluenga, K. B. Hueso, J. C. Gonzalez and T. Rojo, *Energy Environ. Sci.*, 2012, **5**, 5884.

[32] M. D. Slater, D. H. Kim, E. Lee and C. S. Johnson, *Adv. Funct. Mater.*, 2013, **23**, 947.

[33] C. N. R. Rao, A. K. Sood, K. S. Subrahmanyam and A. Govindaraj, *Angew. Chem. Int. Ed.*, 2009, **48**, 7752.
[34] V. Wang, H. Mizuseki, H. P. He, G. Chen, S. L. Zhang and Y. Kawazoe, *Comp. Mater. Sci.*, 2012, **55**, 180.
[35] A. Lherbier, A. R. Botello-Méndez and J. C. Charlier, *Nano Lett.*, 2013, **13**, 1446.
[36] A. H. Castro Neto, F. Guinea, N. M. R. Peres, K. S. Novoselov and A. K. Geim, *Rev. Mod. Phys.*, 2009, **81**, 109.
[37] E. J. Yoo, J. Kim, E. Hosono, H. S Zhou, T. Kudo and I. Honma, *Nano Lett.*, 2008, **8**, 2277.
[38] G. X. Wang, X. P. Shen, J. Yao and J. Park, *Carbon*, 2009, **47**, 2049.
[39] Y. Q. Sun, Q. Wu and G. Q. Shi, *Energy Environ. Sci.*, 2011, **4**, 1113-1132.
[40] X. Huang, X. Y. Qi, F. Boey and H. Zhang, *Chem. Soc. Rev.*, 2012, **41**, 666.
[41]D. A. Stevens and J. R. Dahn, *J. Electrochem. Soc*, 2000, **147**, 1271.
[42] Y. X. Wang, S. L. Chou, H. K. Liu and S. X. Dou, *Carbon*, 2013, **57**, 202.
[43] D. Datta, J. W. Li and V. B. Shenoy, *ACS Appl. Mater. Interfaces*, 2014, **6**, 1788.
[44] Y. Yan, Y. X. Yin, Y. G. Guo and L. J. Wan, *Adv. Energy Mater.*, 2014, **4**, 1301584.
[45] P. Simon and Y. Gogotsi, *Acc. Chem. Res.*, 2013, **46**, 1094.
[46] D. Y. W. Yu, P. V. Prikhodchenko, C. W. Mason, S. K. Batabyal, J. Gun, S. Sladkevich, A. G. Medvedev and O. Lev, *Nat. Commun.*, 2013, **4**, 2922.
[47] L. David, R. Bhandavat and G. Singh, *ACS Nano*, 2014, **8**, 1759.
[48] S. C. Lyu, J. H. Han, K. W. Shin and J. H. Sok, *Carbon*, 2011, **49**, 1532.
[49] L. G. Bulusheva, A. V. Okotrub, A. G. Kurenya, H. K. Zhang, H. J. Zhang, X. H. Chen and H. H. Song, *Carbon*, 2011, 4013.
[50] X. F. Li, D. S. Geng, Y. Zhang, X. B. Meng, R. Y. Li and X. L. Sun, *Electrochem. Commun.*, 2011, **13**, 822.
[51] W. H. Shin, H. M. Jeong, B. G. Kim, J. K. Kang and J. W. Choi, *Nano Lett.*, 2012, **12**, 2283.
[52] Y. S. Yun, V. D. Le, H. Kim, S. J. Chang, S. J. Baek, S. J. Park, B. H. Kim, Y. H. Kim, K. Kang and H. J. Jin, *J. Power Sources*, 2014, **262**, 79.
[53] L. S. Panchakarla, K. S. Subrahmanyam, S. K. Saha, A. Govindaraj, H. R. Krishnamurthy, U. V. Waghmare and C. N. R. Rao, *Adv. Mater.*, 2009, **21**, 4726.
[54] X. L. Wang, Z. Zeng, H. J. Ahn and G. X. Wang, *Appl. Phys. Lett.*, 2009, **95**, 183103.
[55] T. Liu, R. Y. Luo, S. H. Yoon and I. Mochida, *J. Power Sources*, 2010, **195**, 1714.
[56] Z. S. Wu, W. C. Ren, L. Xu, F. Li and H. M. Cheng, *ACS Nano*, 2011, **5**, 5463.
[57] C. C. Ma, X. H. Shao, D. P. Cao, *J. Mater. Chem.*, 2012, **22**, 8911.
[58] H. B. Wang, C. J. Zhang, Z. H. Liu, L. Wang, P. X. Han, H. X. Xu, K. J. Zhang, S. M. Dong, J. H. Yao and G. L. Cui, *J. Mater. Chem.*, 2011, **21**, 5430.
[59] R. F. Lu, D. W. Rao, Z. L. Lu, J. C. Qian, F. Li, H. P. Wu, Y. Q. Wang, C. Y. Xiao, K. M. Deng, E. J. Kan and W. Q. Deng, *J. Phys. Chem. C*, 2012, **116**, 21291.
[60] D. W. Rao, R. F. Lu, Z. S. Meng, Y. H. Wang, Z. L. Lu, Y. Z. Liu, X. Chen, E. J. Kan, C. Y. Xiao, K. M. Deng and H. P. Wu, *Int. J. Hydrogen Energy,* 2014, **39**, 18966.
[61] R. F. Lu, Z. S. Meng, E. J. Kan, F. Li, D. W. Rao, Z. L. Lu, J. C. Qian, C. Y. Xiao, H. P. Wu and K. M. Deng, *Phys. Chem. Chem. Phys.*, 2013, **15**, 666.
[62] R. F. Lu, D. W. Rao, Z. S. Meng, X. B. Zhang, G. J. Xu, Y. Z. Liu, E. Kan, C. Y. Xiao and K. M. Deng, *Phys. Chem. Chem. Phys.*, 2013, **15**, 16120.
[63] C. Ling and F. Mizuno, *Phys. Chem. Chem. Phys.*, 2014, **16**, 10419.
[64] H. G. Wang, Z. Wu, F. L. Meng, D. L. Ma, X. L. Huang, L. M. Wang and X. B. Zhang, *ChemSusChem.*, 2013, **6**, 56.
[65] L. H. Yao, M. S. Cao, H. J. Yang, X. J. Liu, X. Y. Fang and J. Yuan, *Comp. Mater Sci.*, 2014, **85**, 179.
[66] J. H. Yang, MiRuJo, M. Kang, Y. S. Huh, H. Jung and Y. M. Kang, *Carbon*, 2014, **73**, 106.
[67] Y. P. Lin, Y. Ksari, J. Prakash, L. Giovanelli, J. C. Valmalette, J. M. Themlin, *Carbon*, 2014, **73**, 216.
[68] B. Delley, *J. Chem. Phys.*, 1990, **92**, 508.
[69] B. Delley, J. Chem. Phys., 2000, **113**, 7756.
[70] G. Kresse, J. Furthmüller, *Phys. Rev. B*, 1996, **54**, 11169.
[71] J. P. Perdew, B. Kieron, E. Matthias, *Phys. Rev. Lett.*, 1996, **77**, 3865.
[72] D. W. Rao, R. F. Lu, C. Y. Xiao, E. Kanab and K. M. Deng, *Chem. Commu.*, 2011,47, 7698.
[73] S. Jalili, R. Vaziri, *Mol. Phys.*, 2011, 109, 687.
[74] R. P. Hardikar, D. Das, S. S. Han, K. R. Lee, A. K. Singh, *Phys. Chem. Chem. Phys.*, 2014, **16**, 16502.

Graphical Abstract

Via DFT calculations, we theoretically demonstrated that the N doped defective structures are beneficial for Na binding and that the charge transfer can significantly influence the adsorption energies.